PAPER

NJC
www.rsc.org/njc

Structures and nonlinear optical properties of new symmetrical two-photon photopolymerization initiators†

Yun-Xing Yan,*[a] Xu-Tang Tao,[a] Yuan-Hong Sun,[b] Chuan-Kui Wang,[b] Gui-Bao Xu,[a] Wen-Tao Yu,[a] Hua-Ping Zhao,[a] Jia-Xiang Yang,[a] Xiao-Qiang Yu,[a] Yong-Zhong Wu,[a] Xian Zhao[a] and Min-Hua Jiang[a]

[a] *State Key Laboratory of Crystal Materials, Shandong University, Jinan, 250100, P. R. China. E-mail: yxyan@icm.sdu.edu.cn*

[b] *Department of Physics, Shandong Normal University, Jinan, 250014, P. R. China*

Received (in St. Louis, MO, USA) 3rd October 2004, Accepted 29th November 2004
First published as an Advance Article on the web 2nd February 2005

Four new symmetrical, two-photon photopolymerization initiators, 9-(4-{(1*E*,11*E*)-4-[(*E*)-4-(9*H*-carbazol-9-yl)styryl]-2,5-dimethoxystyryl}phenyl)-9*H*-carbazole (**1**), *N*-(4-{(1*E*,8*E*)-4-[(*E*)-4-(diphenylamino)styryl]-2,5-dimethoxystyryl}phenyl)-*N*-phenylbenzeneamine (**2**), 1,4-bis{2-[4-(2-pyridin-4-ylvinyl)phenyl]vinyl}-2,5-bisdimethoxybenzene (**3**) and 1,4-bis{2-[4-(2-pyridin-4-ylvinyl)phenyl]vinyl}-2,5-bisdodecyloxybenzene (**4**), have been synthesized and characterized. One-photon fluorescence, one-photon fluorescence quantum yields, one-photon fluorescence lifetimes, and two-photon fluorescence have been investigated. The results show that they are all good two-photon absorbing chromophores and effective two-photon photopolymerization initiators. The two-photon absorption cross-sections of these molecules have been evaluated by theoretical calculations. Microfabrication *via* two-photon-initiated polymerization has been studied and the possible photopolymerization mechanism is discussed.

1. Introduction

Organic materials possessing large two-photon absorption (TPA) cross sections can be used for a variety of technical applications, such as in three-dimensional (3D) optical data storage and microfabrication,[1–8] optical power limiting,[9,10] localized photodynamic therapy,[11] and two-photon laser scanning fluorescence imaging.[12–14] In TPA, the absorption transition probability is proportional to the square of the incident intensity. This quadratic dependence of TPA on light intensity limits the absorption process to the immediate vicinity of the focal point, providing a large penetration depth and a high resolution of the excitation volume. Thus, TPA-initiated photopolymerization appears to be an interesting method for the fabrication of complex micrometer-sized 3D structures with high resolution in one step. When a chromophore, acting as a polymerization photoinitiator, is excited by simultaneous absorption of two photons, it can lead to the formation of solid structures in the presence of a monomer. To be efficient initiators of the chain reaction with acrylates, the selected compounds must have a large TPA cross section and must be able to produce radicals upon excitation.

Much effort has been expended to develop efficient two-photon chromophores by use of either a symmetrically or asymmetrically substituted π-conjugated unit.[15–18] Recent research encompassing synthesis, structures and theory has revealed the importance of certain basic structural motifs for TPA-active organic materials.[19–21] In particular, a framework for mobile π electrons with electron donor and acceptor groups on the terminal sites, with or without donors/acceptors in the middle of the conjugated framework, provides the potential for symmetric charge displacement upon excitation and enhanced TPA. However, effective initiators are still rare as the relation between the structures and properties required for initiating two-photon photopolymerization remains unclear. In this contribution, we present the synthesis, characterization and calculated two-photon cross sections of a series of symmetrical chromophores, namely 9-(4-{(1*E*,11*E*)-4-[(*E*)-4-(9*H*-carbazol-9-yl)styryl]-2,5-dimethoxystyryl}phenyl)-9*H*-carbazole (**1**), *N*-(4-{(1*E*,8*E*)-4-[(*E*)-4-(diphenylamino)styryl]-2,5-dimethoxystyryl}phenyl)-*N*-phenylbenzeneamine (**2**), 1,4-bis{2-[4-(2-pyridin-4-ylvinyl)phenyl]vinyl}-2,5-bisdimethoxybenzene (**3**) and 1,4-bis{2-[4-(2-pyridin-4-ylvinyl)phenyl]vinyl}-2,5-bisdodecyloxybenzene (**4**). Compared to the known two-photon photopolymerization initiators,[2] the acceptor groups are attached to the ends of **3** and **4**. Our results demonstrate that they are all good two-photon absorbing chromophores and effective two-photon photopolymerization initiators.

It should be mentioned that, although **1** and some related compounds have been synthesized previously,[22–25] its crystal structure, one-photon fluorescence lifetime and calculated two-photon cross section have not been previously investigated. Moreover, the use of **1–4** as initiators had not been studied.

2. Experimental

2.1. Chemicals and instruments

4-Carbazol-9-ylbenzaldehyde was synthesized according to the reported methods.[26] Triphosphonium chloride (**1′**) was synthesized by our laboratory. 4-Bromobenzyl(triphenyl)phosphonium bromide (**2′**) and 2,5-bisdodecyloxybenzene-1,4-dicarbaldehyde (**3′**) were synthesized according to the literature methods.[27,28] The 600 MHz H^1 NMR and ^{13}C NMR spectra were obtained on a Bruker av600 spectrometer. Elemental analyses were performed using a PE2400 elemental analyzer. UV-Vis-near-IR spectra were measured on a Hitachi

† Electronic supplementary information (ESI) available: NMR spectra of **1** and **2**. Packing diagram of **1**. The linear absorption and the one- and two-photon fluorescence spectra of **1–4**. See http://www.rsc.org/suppdata/nj/b4/b415354e/

DOI: 10.1039/b415354e

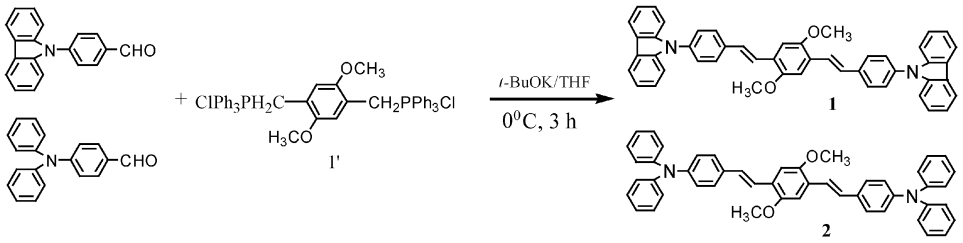

Scheme 1 Synthesis of **1** and **2**.

U-3500 recording spectrophotometer. Melting points were measured on DSC822[e] Mettler–Toledo instruments.

The linear absorption spectra were measured in solvents of different polarity at a concentration of $c = 1 \times 10^{-5}$ mol l^{-1}, and the solvent influence eliminated. The steady-state fluorescence spectra measurements were performed with an Edinburgh FLS 920 spectrofluorimeter. A 450 W Xe arc lamp provided the ~400 nm excitation radiation. The one-photon fluorescence spectra were measured with the same concentrations as those of the linear absorption spectra. The maximum one-photon fluorescence excitation wavelengths for **1**, **2**, **3** and **4** are 400, 420, 420 and 430 nm, respectively. The two-photon fluorescence spectra were observed with a laser beam from a mode-locked Ti:sapphire laser (Coherent Mira 900F) as the pump source with a pulse duration of 200 fs, a repetition rate of 76 MHz, and a single-scan streak camera (Hamamatsu Model C5680-01), together with a monochromator as the recorder. The excitation wavelengths of **1**, **2**, **3** and **4** were 760, 820, 830 and 830 nm, respectively. The concentration was $c = 1 \times 10^{-3}$ mol l^{-1}.

2.2. Synthesis and structure

The synthetic approaches for **1** and **2** and for **3** and **4** are shown in Schemes 1 and 2, respectively.

9-(4-{(1*E*,11*E*)-4-[(*E*)-4-(9*H*-Carbazol-9-yl)styryl]-2,5-dimethoxystyryl}phenyl)-9*H*-carbazole (1). Under argon atmosphere, **1′** (1 mmol) and 4-carbazol-9-ylbenzaldehyde (2 mmol) were dissolved in dry THF (100 ml) at 0 °C. Potassium *tert*-butoxide (3 mmol) was then added portion-wise and the reaction mixture was allowed to stand for 2 h. This mixture was then ground and poured into distilled water (200 ml), neutralized with dilute hydrochloric acid, and extracted with dichloromethane. The organic layer was then dried over anhydrous magnesium sulfate and evaporated to yield a green powder, which was further purified by column chromatography on silica gel using ethyl acetate–petroleum benzine (1 : 10) as eluent and crystallized using ethyl acetate with a yield of 35% and a mp 204.8 °C. The enthalpy is −71.76 mJ mg^{-1}. Anal. calcd for $C_{48}H_{36}N_2O_2$: C, 85.71; H, 5.36; N, 4.17; found: C, 85.98; H, 5.44; N, 4.23%. ^{1}H NMR (600 MHz, $CDCl_3$) δ: 8.17 (d, 4H, J = 7.6 Hz), 7.79 (d, 2H, J = 7.8 Hz), 7.58 (q, 6H, J = 7.3 Hz), 7.43 (m, 10H), 7.30 (q, 4H, J = 7.1 Hz), 7.23 (d, 1H, J = 12.5 Hz), 6.94 (d, 1H, J = 12.4 Hz), 6.89 (d, 1H, J = 12.1 Hz), 6.80 (d, 1H, J = 12.2 Hz), 3.97 (s, 3H), 3.66 (s, 3H). ^{13}C NMR (600 MHz, $CDCl_3$) δ: 153.23, 152.40, 142.32, 142.25, 138.51, 138.25, 137.90, 131.89, 131.01, 130.92, 129.67, 129.36, 128.67, 128.15, 127.84, 127.72, 127.60, 127.44, 127.31, 125.67, 124.93, 122.24, 121.86, 121.81, 121.50, 121.47, 114.87, 111.34, 111.14, 110.48, 57.78, 57.51.

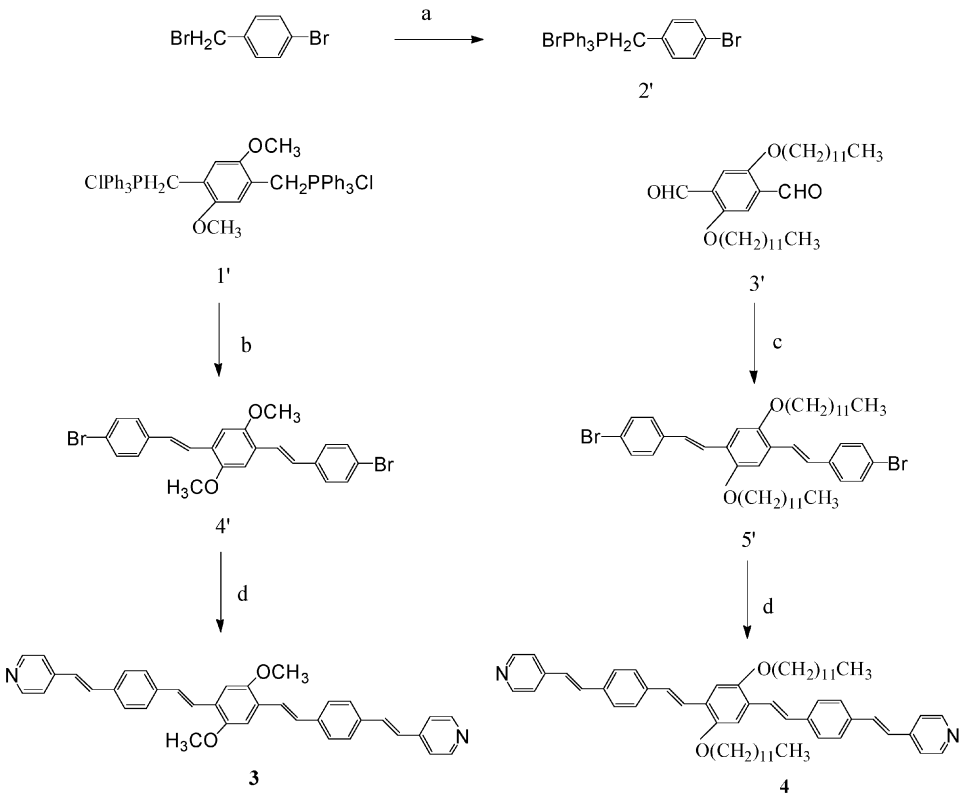

Scheme 2 Synthesis of **3** and **4**: (a) PPh_3, CCl_4, BPO, reflux; (b) THF, 4-bromobenzaldehyde, grinding, RT; (c) THF, **2′**, grinding, RT; (d) vinylpyridine, tri-*o*-tolylphosphine, palladium(II) acetate, triethylamine, reflux.

***N*-(4-{(1*E*,8*E*)-4-[(*E*)-4-(Diphenylamino)styryl]-2,5-dimethoxystyryl}phenyl)-*N*-phenylbenzeneamine (2).** Compound **2** was obtained by a similar method for **1**. It forms orange needle-like crystals (yield 38%). Anal. calcd for $C_{48}H_{40}N_2O_2$: C, 85.18; H, 5.96; N, 4.14; found: C, 85.69; H, 6.02; N, 4.19%. ^{1}H NMR (600 MHz, $CDCl_3$) δ: 7.45 (d, 4H, J = 8.45), 7.41 (s, 1H), 7.38 (s, 1H), 7.28 (q, 6H, J = 8.03 Hz), 7.14 (d, 11H, J = 8.14 Hz), 7.07 (m, 11H), 3.93 (s, 6H). ^{13}C NMR (600 MHz, $CDCl_3$) δ: 152.96, 149.09, 148.69, 133.70, 130.76, 129.80, 128.92, 128.17, 125.94, 125.16, 124.46, 123.19, 110.50, 57.92.

1,4-Bis{2-[4-(2-pyridin-4-ylvinyl)phenyl]vinyl}-2,5-bisdimethoxybenzene (3). At room temperature, 4-bromobenzaldehyde (1.85 g, 0.01 mol), **1′** (3.16 g, 0.004 mol), NaOH (8.00 g, 0.2 mol) and THF (2 ml) were added into a mortar. The mixture was ground for 5 min, then poured into distilled water (200 ml), neutralized with dilute hydrochloric acid, and extracted with dichloromethane. The organic layer was dried over anhydrous magnesium sulfate. After filtration, the solvent was removed at reduced pressure and the residue was dissolved in dichloromethane. The resulting solution was chromatographed on silica gel using ethyl acetate–petroleum ether (1 : 20) as eluent. Then the isolated green crystals were added into a mixture of tri-*o*-tolylphosphine (1.96 g, 6.44 mmol), vinylpyridine (3.48 ml, 32.24 mmol), palladium(II) acetate (0.18 g, 0.8 mmol) and redistilled triethylamine (100 ml). The mixture was refluxed in an oil bath under nitrogen, giving an orange solution after heating and stirring for 36 h. The solvent was removed under reduced pressure and the residue was dissolved in methylene chloride, washed three times with distilled water, and dried with anhydrous magnesium sulfate. Then it was filtered and concentrated. The resulting solution was chromatographed on silica gel using ethyl acetate as eluent. The final product was obtained as a red solid (yield 34%). Anal. calcd for $C_{38}H_{32}N_2O_2$: C 83.21, H 5.84, N 5.11; found: C 83.97, H 5.95, N 5.23%. ^{1}H NMR ($CDCl_3$, 600 MHz) δ: 8.58 (4H, q, J = 5.2 Hz), 7.56 (3H, q, J = 10.9 Hz), 7.44 (3H, t, J = 7.6 Hz), 7.36 (7H, m), 7.15 (1H, t, J = 9.1 Hz), 7.02 (4H, d, J = 16.2 Hz), 6.80 (2H, d, J = 7.3 Hz), 6.75 (2H, t, J = 12.3 Hz), 6.66 (2H, t, J = 12.8 Hz), 3.90 (3H, s), 3.54 (3H, s). ^{13}C NMR (600 MHz, $CDCl_3$) δ: 152.26, 151.64, 146.26, 146.10, 139.89, 139.57, 136.35, 134.49, 134.28, 131.34, 131.24, 130.97, 129.90, 128.89, 128.50, 128.29, 128.26, 127.75, 127.53, 127.43, 127.21, 127.14, 125.38, 122.30, 122.26, 114.82, 114.34, 110.31, 57.71, 57.44.

1,4-Bis{2-[4-(2-pyridin-4-ylvinyl)phenyl]vinyl}-2,5-bisdodecyloxybenzene (4). This was obtained by a similar approach as for **3** (yield 39%). Anal. calcd for $C_{60}H_{76}N_2O_2$: C 84.11, H 8.88, N 3.27; found: C 84.79, H 8.97, N 3.35%. ^{1}H NMR ($CDCl_3$, 600 MHz) δ: 8.59 (4H, d, J = 4.0 Hz), 7.57 (10H, m), 7.41 (4H, d, J = 4.7 Hz), 7.36 (1H, s), 7.33 (1H, s), 7.19 (1H, s), 7.15 (3H, d, J = 2.2 Hz), 7.05 (2H, d, J = 16.2 Hz), 4.09 (4H, t, J = 6.4 Hz), 1.91 (4H, m), 1.58 (4H, m), 1.41 (32H, m), 0.88 (6H, t, J = 6.8 Hz). ^{13}C NMR (600 MHz, $CDCl_3$) δ: 151.25, 149.62, 138.69, 135.11, 133.29, 128.22, 127.47, 126.97, 125.39, 124.25, 120.92, 114.58, 114.39, 110.71, 69.62, 31.92, 29.72, 29.68, 29.64, 29.58, 29.50, 29.46, 29.38, 26.32, 22.68, 14.10.

X-Ray crystallography

The X-ray diffraction data of **1** were collected using a Bruker P4 four-circle diffractometer with MoKα radiation. The number of measured reflections was 4161, of which 3936 were independent (R_{int} = 0.0354). The structure was solved by direct methods and refined with least-squares techniques using SHELXL-97 programs.[29] Crystal data for **1**: $C_{48}H_{36}N_2O_2$, FW = 672.79, monoclinic system, space group Pc, μ = 0.074 mm^{-1}, a = 8.777(5), b = 21.279(5), c = 9.934(5) Å, β = 97.797(5)°, Z = 2, U = 1838.2(15) Å^3, T = 293(2) K, D_c = 1.216 g cm^{-3}, R_1 = 0.0648, wR_2 = 0.1199 for $I > 2\sigma(I)$.‡

3. Results and discussion

3.1. Structure and characterization

Selected bond lengths and bond angles of **1** are given in Table 1. The bond lengths of all single bonds are significantly shorter than the typical single bonds, whereas the double bonds are significantly longer than typical double bonds. The bond lengths of the phenyl ring and carbazole ring are all of normal aromatic character. These structural features indicate that **1** has a π-conjugated system although the planarity is not very good. Indeed, the dihedral angles between two carbazole rings and their adjacent phenyl rings are 126.3 and 51.8°, respectively. The dihedral angles between the central phenyl ring and the adjacent two phenyl rings are 113.9 and 55.7°, respectively. The apparently centrosymmetrical **1** is, in fact, rather asymmetrical, as illustrated in Fig. 1. In the crystal structure, the chemical surroundings of the H atoms on C27 and C28 are different, which may be responsible for the different chemical shifts of the hydrogens on C27 and C28 in the ^{1}H NMR spectra, as well as explain the different numbers of carbon atoms, 32 *versus* 16, in the ^{13}C NMR spectra. These characteristics in the ^{1}H NMR and ^{13}C NMR spectra have also been observed for **3**. In contrast, the ^{1}H NMR and ^{13}C NMR spectra of **2** and **4** indicate that they are centrosymmetric. The ^{1}H NMR spectra of **1** and **2** are given in the ESI.

3.2. One- and two-photon fluorescence

The photophysical properties of these compounds are summarized in Table 2. The linear absorption, one-photon fluorescence and two-photon fluorescence spectra of these compounds are shown in the ESI. The linear absorption and fluorescence spectra in DMF for **1** are depicted in Fig. 2.

As shown in Table 2, the absorption maxima are not significantly different, while the fluorescence maxima are slightly red-shifted and the fluorescent lifetimes are lengthened upon increasing the polarity of the aprotic solvent for **2**, **3** and **4**. This can be explained by a possibly higher polarity for the excited states than for the ground states, since solvatochromism is associated with energy level lowering. Increased dipole–dipole interactions between the solute and solvent lower the energy levels greatly.[30,31] In the case of benzyl alcohol, the possibility of hydrogen bonding between the solvent and solute molecules will push the excitation energy even lower.[32] For **1**, the absorption/fluorescence maxima show no obvious change with an increase in polarity of the aprotic solvent. The maxima (Table 2) of the two-photon fluorescence show slight red-shifts compared to the one-photon fluorescence in the same solvent for each compound. This can be ascribed to the effect of re-absorption as the linear absorption band has a slight overlap with the emission band and our two-photon fluorescence experiments were carried out on concentrated solutions that made re-absorption a significant process.[33] The absorption/fluorescence maxima of **2** show an obvious red-shift, and the one-photon quantum yield indicate an obvious increase compared to **1** in each solvent. This can be explained by the facts that the structure of **2** is centrosymmetric and possesses excellent planarity, compared to **1**, and that the electron donating strength of diphenylamino is greater than that of carbazolyl. Compared to **3**, the fluorescence maximum of **4** shows a slight red-shift and the one-photon quantum yield shows no obvious change compared to **3** in each solvent. This implies that the substituents on the O atom have no significant influence on the properties for these two molecules.

‡ CCDC reference number 261654. See http://www.rsc.org/suppdata/nj/b4/b415354e/ for crystallographic data in .cif or other electronic format.

Table 1 Selected bond lengths (Å) and bond angles (°) for molecule **1**

C1–N1	1.368(8)	C16–(17	1.375(9)	C32–C33	1.374(10)
C1–C2	1.3900	C16–C19	1.468(10)	C33–C34	1.393(10)
C1–C6	1.3900	C17–C18	1.381(10)	C34–C35	1.383(10)
C2–C3	1.3900	C19–C20	1.339(9)	C34–N2	1.423(10)
C3–C4	1.3900	C20–C21	1.462(10)	C35–C36	1.366(10)
C4–C5	1.3900	C21–C22	1.399(10)	C37–C38	1.3900
C5–C6	1.3900	C21–C26	1.413(11)	C37–C42	1.3900
C6–C7	1.435(9)	C22–C23	1.367(11)	C37–N2	1.390(7)
C7–C8	1.3900	C22–O1	1.390(9)	C38–C39	1.3900
C7–C12	1.3900	C23–C24	1.373(11)	C39–C40	1.3900
C8–C9	1.3900	C24–C25	1.406(11)	C40–C41	1.3900
C9–C10	1.3900	C24–C29	1.469(11)	C41–C42	1.3900
C10–C11	1.3900	C25–O2	1.354(10)	C42–C43	1.422(7)
C11–C12	1.3900	C25–C26	1.378(10)	C43–C44	1.3900
C12–N1	1.372(8)	C27–O2	1.424(10)	C43–C48	1.3900
C13–C18	1.373(10)	C28–O1	1.413(9)	C44–C45	1.3900
C13–C14	1.381(9)	C29–C30	1.329(10)	C45–C46	1.3900
C13–N1	1.402(9)	C30–C31	1.480(11)	C46–C47	1.3900
C14–C15	1.379(9)	C31–C32	1.374(9)	C47–C48	1.3900
C15–C16	1.391(10)	C31–C36	1.386(10)	C48–N2	1.360(8)
N1–C1–C6	109.9(6)	C16–C17–C18	120.4(8)	C32–C33–C34	118.4(8)
C2–C1–C6	120.0	C15–C16–C19	122.2(7)	C35–C34–C33	120.2(8)
C3–C2–C1	120.0	C13–C18–C17	121.0(7)	C39–C40–C41	120.0
C1–C6–C7	107.1(6)	C20–C19–C16	125.3(8)	C42–C41–C40	120.0
C12–C7–C6	105.0(7)	C26–C25–C24	119.7(9)	C47–C46–C45	120.0
C7–C8–C9	120.0	C25–C26–C21	121.1(8)	N2–C48–C47	129.9(6)
C18–C13–C14	118.7(8)	C32–C31–C36	118.5(8)	N2–C48–C43	110.1(6)
C17–C16–C19–C20	−149.6(8)	C11–C12–N1–C13	5.0(10)	C18–C13–N1–C1	−51.6(11)
C16–C19–C20–C21	177.6(7)	C24–C29–C30–C31	7.9(18)	C38–C37–N2–C34	−6.7(10)
C19–C20–C21–C26	36.6(12)	C29–C30–C31–C36	31.9(16)	C33–C34–N2–C37	−51.5(11)
C23–C24–C29–C30	46.0(15)	C2–C1–N1–C13	−8.8(10)	C29–C30–C31–C32	−152.0(11)

3.3. Two-photon absorption cross section

The transition intensity for one-photon absorption (OPA) is described by an oscillator strength:

$$\delta_{\mathrm{op}} = \frac{2\omega_f}{3}\sum_{\alpha}|\langle 0|\mu_\alpha|f\rangle|^2 \mathrm{X} \qquad (1)$$

where μ_α is the electric dipole moment operator, ω_f denotes the excitation energy of the excited state $|f\rangle$, $|0\rangle$ denotes the ground state, and the summation is performed over α, the molecular x, y and z axes.

In terms of the sum-over-state formula, the two-photon matrix element for the two-photon resonant absorption of two photons with identical energy is written as:

$$S_{\alpha\beta} = \sum_j \left[\frac{\langle 0|\mu_\alpha|j\rangle\langle j|\mu_\beta|f\rangle}{\omega_j - \omega_f/2} + \frac{\langle 0|\mu_\beta|j\rangle\langle j|\mu_\alpha|f\rangle}{\omega_j - \omega_f/2}\right] \qquad (2)$$

Where $|0\rangle$ and $|f\rangle$ denote the ground state and the final state, respectively. $|j\rangle$ denotes all the intermediate states, including the ground state. ω_j is the excitation energy of the excited state $|j\rangle$. The TPA cross section is given by orientational averaging over the two-photon absorption probability:

$$\delta_{\mathrm{tpa}} = \sum_{\alpha\beta}\left[F \times S_{\alpha\alpha}S^*_{\beta\beta} + G \times S_{\alpha\beta}S^*_{\alpha\beta} + H \times S_{\alpha\beta}S^*_{\beta\alpha}\right] \qquad (3)$$

where the coefficients F, G and H are related to the incident radiation. For linearly polarized light, F, G and H are 2, 2 and 2, but for the circularly polarized case, they are −2, 3 and 3, respectively. In this work, we only consider the results with a linearly polarized laser beam. The summation goes over the molecular axes α, $\beta = \{x, y, z\}$.

The TPA cross section directly comparable with the experimental measurements is defined as:

$$\sigma_{\mathrm{tpa}} = \frac{4\pi^2 a_0^5 \alpha}{15 c_0}\frac{\omega^2 g(\omega)}{\Gamma_f}\delta_{\mathrm{tpa}} \qquad (4)$$

where a_0 is the Bohr radius, c_0 is the speed of light, α is the fine structure constant, ω is the photon energy of the incident light, $g(\omega)$ denotes the spectral line profile (here it was assumed to be a δ function). Γ_f is the lifetime broadening of the final state, which was assumed to be 0.1 eV.[19]

The GAUSSIAN-98 program package[36] was utilized to optimize the molecular geometrical structure with the hybrid density functional theory (DFT/B3LYP) and a 6-31G basis set. The program DALTON[37] was used to calculate the one-photon absorption strength and TPA cross sections of these molecules with response function theory in the random phase approximation. The maximum absorption strength for the one-photon case takes place in the first excited state. The maximum TPA cross sections for compounds **1**, **2** and **3** occur for the second excited state and are 1.54, 2.36 and 0.73×10^{-48} cm^4 s photon^{-1}, respectively. For **4**, due to the large number of atoms, we were unable to optimize completely the structure and hence were unable to obtain the two-photon cross section. For the first excited state, the TPA cross sections are smaller

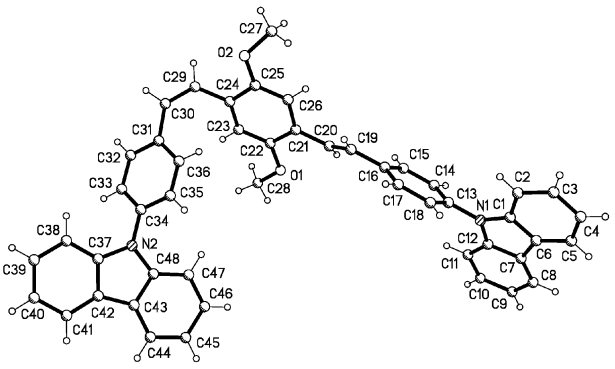

Fig. 1 Crystal molecular structure of **1**.

Table 2 Data from the absorption and the one- and two-photon fluorescence spectra, showing the solvent effects

Compound	Solvent	ε^a	$\lambda_{max}^{(1a)\,b}$/nm	$\varepsilon_{res}/10^4$	$\lambda_{max}^{(1f)\,b}$/nm	τ^c/ns	Φ^d	$\lambda_{max}^{(2f)\,b}$/nm
1	DMF	37.6	401	7.35	458	1.36	0.48	466
	CH_2Cl_2	9.1	402	6.79	458	1.33	0.44	462
	Benzyl alcohol	13.1	408	6.83	462	1.23	0.54	468
	THF	7.58	403	6.84	458	1.31	0.42	464
	$CHCl_3$	4.806	404	6.63	458	1.27	0.41	462
2	DMF	37.6	426	5.52	510	1.46	0.67	516
	CH_2Cl_2	9.1	427	5.26	496	1.33	0.60	506
	Benzyl alcohol	13.1	431	4.30	500	1.27	0.71	510
	THF	7.58	421	4.20	494	1.30	0.58	503
	$CHCl_3$	4.806	423	4.70	492	1.21	0.59	500
3	DMF	37.6	415	4.36	518	1.67	0.66	
	CH_2Cl_2	9.1	419	6.02	512	1.56	0.63	
	Benzyl alcohol	13.1	429	5.51	520	1.42	0.76	
	THF	7.58	420	6.62	510	1.52	0.60	
	$CHCl_3$	4.806	423	5.78	506	1.41	0.66	525
4	DMF	37.6	421	3.52	520	1.65	0.65	
	CH_2Cl_2	9.1	425	5.38	514	1.43	0.61	
	Benzyl alcohol	13.1	433	4.87	522	1.52	0.75	
	THF	7.58	426	5.54	512	1.38	0.58	
	$CHCl_3$	4.806	428	5.00	508	1.35	0.63	529

[a] ε is the relative permittivity measured at 20 °C.[34] ε_{res} is the corresponding molar absorption coefficient. [b] $\lambda_{max}^{(1a)}$, $\lambda_{max}^{(1f)}$ and $\lambda_{max}^{(2f)}$ are the one-photon absorption, one-photon fluorescence and two-photon fluorescence maxima peak, respectively. [c] τ is the one-photon fluorescence lifetime. [d] Φ is the one-photo quantum yield determined using Coumarin 307 as the standard.[35]

compared to the maximum values but are finite. Therefore, the fluorescent spectra by TPA for the first excited state can still be observed.

3.4. Two-photon photopolymerization

Our two-photon-initiated photopolymerization experiments have been carried out using **1–4** as initiators, with wavelengths of 760, 820, 830 and 830 nm, respectively. The 2D lattice was fabricated with a negative resin system, which contained an oligomer (bisphenyl A epoxide dimethylacrylate), 5% of the initiator and a small amount of dichloroethane (to increase the compatibility and control the viscosity). The same mode-locked Ti:sapphire laser as that used in the two-photon fluorescence measurements was used for two-photon microfabrication. The lasing source was tightly focused *via* an objective lens (×40, NA = 0.65) and the focal point was focused on the sample film place on the *xy*-step motorized stage controlled by computer. The pulse energy, after being focused by the objective lens, was ~20 mW. The polymerized solid skeleton was obtained after the unreacted liquid mixture had been washed out. The fabricated lattice was observed through a polarization microscope (Olympus, BX-51), as illustrated in Fig. 3. Fig. 3 shows a 0.08 × 0.06 mm polymerization region with a two dimensional structure. The distance between two neighboring polymerization streaks is about 8 μm.

The photopolymerization mechanism of these initiators is still unknown. According to Cumpston *et al.*[2] strong donor substituents would make the conjugated system electron-rich, and after one- or two-photon photoexcitation, the molecule would be able to transfer an electron even to relatively weak acceptors; this process could be used to activate the polymerization reaction. In order to demonstrate this process, we performed *ab initio* calculations at the time-dependent hybrid density functional theory B3LYP level coded in the GAUSSIAN-98 program package for **2**, showing that the first excited state is the charge-transfer (CT) state with an excitation energy λ = 541 nm. When the molecule is irradiated by the 820 nm laser, it can be expected that the molecule will simultaneously absorb two photons and be excited to the first excited state (the CT state). For a better understanding of the charge-transfer process, the charge density difference between the ground and the CT states in a molecule of **2** in the gas phase is depicted in Fig. 4.[38] It is clear that upon excitation, charge is mainly

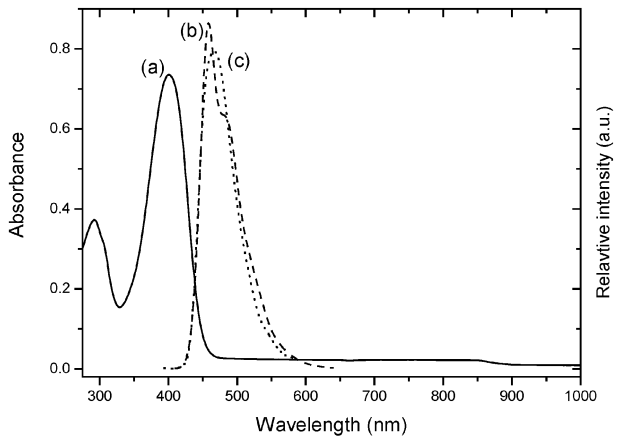

Fig. 2 Absorption and fluorescence spectra of **1**. Curves a and b are the linear absorption and one-photon fluorescence spectra, respectively, with $c = 1 \times 10^{-5}$ mol l^{-1} in DMF. Curve c is the two-photon fluorescence spectra with $c = 1 \times 10^{-3}$ mol l^{-1} in DMF.

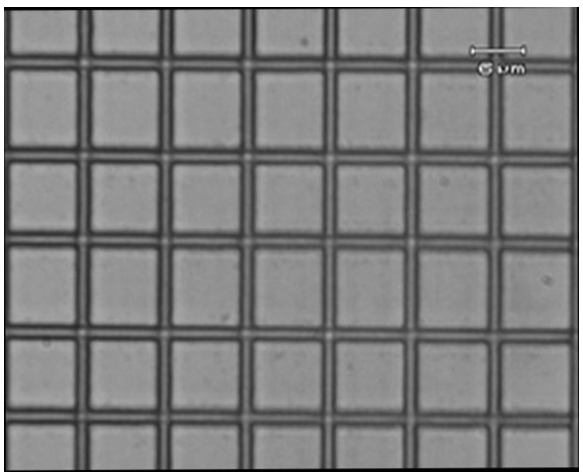

Fig. 3 Optical micrograph of the lattice fabricated *via* two-photon polymerization using **2** as an initiator.

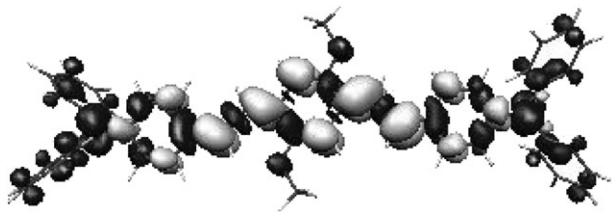

Fig. 4 Density difference between the charge-transfer and ground states of **2** in the gas phase. The light and dark areas represent the electron loss and gain regions, respectively, upon excitation.

distributed at the two terminals of **2**, indicating that it can give away its electron to its surroundings. This result is in accord with the conclusion of Cumpston *et al.*[2] However, whether the photoinduced electron-transfer reaction is energetically feasible needs further theoretical investigation.

4. Conclusions

Four symmetrical two-photon photopolymerization initiators were synthesized and characterized. The crystal structure of **1** has been determined by X-ray single crystal diffraction analysis, showing an asymmetric character. A similar asymmetry can be observed for **3**. For **2** and **4**, the ^{1}H NMR and ^{13}C NMR spectra indicate that they are centrosymmetric. The photophysical results illustrate that the four compounds are all good two-photon absorbing chromophores and effective two-photon photopolymerization initiators. The wavelengths for initiating two-photon polymerization reactions of **1**, **2**, **3** and **4** are 760, 820, 830 and 830 nm, respectively. A possible mechanism is based on a charge-transfer process when the laser irradiation is applied.

Acknowledgements

This work was supported by financial support from the National Natural Science Foundation of China (grant no. 50323006, 50325311, 10274044) and the Swedish International Development Cooperation Agency (SIDA). The authors also thank Prof. Xiao-Ming Chen for his help in revising the manuscript.

References

1 M. Saruo, O. Nakamura and S. Kawata, *Opt. Lett.*, 1997, **22**, 132.
2 B. H. Cumpston, S. P. Ananthavel, S. Barlow, D. L. Dyer, J. E. Ehrlich, L. L. Erskine, A. A. Keikal, S. M. Kuebler, I.-Y. S. Lee, D. M. Maughon, J. Qin, H. Röckel, M. Rumi, X. L. Wu, S. R. Marder and J. W. Perry, *Nature (London)*, 1999, **398**, 51.
3 S. Kawata, H.-B. Sun, T. Tanaka and K. Takada, *Nature (London)*, 2001, **412**, 697.
4 W. Zhou, S. M. Kuebler, K. L. Braun, T. Yu, J. K. Cammack, C. K. Ober, J. W. Perry and S. R. Marder, *Science*, 2002, **296**, 1106.
5 D. A. Parthenopoulos and P. M. Rentzepis, *Science*, 1989, **245**, 843.
6 J. H. Strickler and W. W. Webb, *Opt. Lett.*, 1991, **16**, 1780.
7 A. S. Dvornikov and P. M. Rentzepis, *Opt. Commun.*, 1995, **119**, 341.
8 K. D. Belfield, Y. Liu, R. A. Negres, M. Fan, G. Pan, D. J. Hagan and F. E. Hernandez, *Chem. Mater.*, 2002, **14**, 3663.
9 J. E. Ehrlich, X. L. Wu, L.-Y. Lee, Z.-Y. Hu, H. Roeckel, S. R. Marder and J. Perry, *Opt. Lett.*, 1997, **22**, 1843.
10 G. S. He, G. C. Xu, P. N. Prasad, B. A. Reinhardt, J. C. Bhatt and A. G. Dillard, *Opt. Lett.*, 1995, **20**, 435.
11 J. D. Bhawalkar, N. D. Kumar, C. F. Zhao and P. N. Prasad, *J. Clin. Laser Med. Surg.*, 1997, **15**, 201.
12 W. Denk, J. H. Strickler and W. W. Webb, *Science*, 1990, **248**, 73.
13 C. Xu, W. R. Zipfel, J. B. Shear, R. M. William and W. W. Webb, *Proc. Natl. Acad. Sci. USA*, 1996, **93**, 10763.
14 D. R. Larson, W. R. Zipfel, R. M. Williams, S. W. Clark, M. P. Bruchez, F. W. Wise and W. W. Webb, *Science*, 2003, **300**, 1434.
15 B. A. Reinhardt, L. L. Brott, S. J. Clarson, A. G. Dillard, J. C. Bhatt, R. Kannan, L. Yuan, G. S. He and P. N. Prasad, *Chem. Mater.*, 1998, **10**, 1863.
16 G. S. He, J. D. Bhawalkar, C. F. Zhao and P. N. Prasad, *Appl. Phys. Lett.*, 1995, **67**, 2433.
17 J. D. Bhawalkar, G. S. He and P. N. Prasad, *Rep. Prog. Phys.*, 1996, **59**, 1041.
18 J. E. Ehrlich, X. L. Wu, L.-Y. Lee, Z.-Y. Hu, H. Roeckel, S. R. Marder and J. Perry, *Opt. Lett.*, 1997, **22**, 1843.
19 M. Albota, D. Beljonne, J.-L. Brédas, J. E. Ehrlich, J.-Y. Fu, A. A. Heikal, S. E. Hess, T. Kogej, M. D. Levin, S. R. Marder, D. McCord-Maughon, J. W. Perry, H. Röckel, M. Rumi, G. Subramaniam, W. W. Webb, X.-L. Wu and C. Xu, *Science*, 1998, **281**, 1653.
20 M. Rumi, J. E. Ehrlich, A. A. Heikal, J. W. Perry, S. Barlow, Z. Hu, D. M. Maughon, T. C. Parker, H. Rockel, S. Thayumanavan, S. R. Marder, D. Beljonne and J.-L. Bredas, *J. Am. Chem. Soc.*, 2000, **122**, 9500.
21 Y.-X. Yan, X.-T. Tao, Y.-H. Sun, G.-B. Xu, C.-K. Wang, J.-X. Yang, X. Zhao and M.-H. Jiang, *J. Solid State Chem.*, 2004, **177**, 3007.
22 M. Sigalov, A. Ben-Asuly, L. Shapiro, A. Ellern and V. Khodorkovsky, *Tetrahedron Lett.*, 2000, **41**, 8573.
23 Z. Kotler, J. Segal, M. Sigalov, A. Ben-Asuly and V. Khodorkovsky, *Synth. Met.*, 2000, **115**, 269.
24 J. Segal, Z. Kotler, M. Sigalov, A. Ben-Asuly and V. Khodorkovsky, *Proc. SPIE-Int. Soc. Opt. Eng.*, 1999, **3796**, 153.
25 M. Silagov, A. Ben-Azuly, L. Shapiro and V. Khodorkovsky, *Mol. Cryst. Liq. Cryst. Sci. Technol., Sect. B*, 2000, **25**, 443.
26 X.-M. Wang, Y.-F. Zhou, W.-T. Yu, C. Wang, Q. Fang, M.-H. Jiang, H. Lei and H.-Z. Wang, *J. Mater. Chem.*, 2000, **10**, 2698.
27 Y. Ren, X.-Q. Yu, D.-J. Zhang, D. Wang, M.-L. Zhang, G.-B. Xu, X. Zhao, Y.-P. Tian, Z.-S. Shao and M.-H. Jiang, *J. Mater. Chem.*, 2002, **12**, 3431.
28 B. Wang and M. R. Wasielewski, *J. Am. Chem. Soc.*, 1997, **119**, 12.
29 G. M. Sheldrick, *SHELXL-97, Program for refinement of crystal structures*, University of Göttingen, Germany, 1997.
30 P. Fromherz, *J. Phys. Chem.*, 1995, **99**, 7188.
31 U. Narang, C. F. Zhao, J. D. Bhawalkar, F. V. Bright and P. N. Prasad, *J. Phys. Chem.*, 1996, **100**, 4521.
32 C.-K. Wang, P. Macak, Y. Luo and H. Ågren, *J. Chem. Phys.*, 2001, **114**, 9813.
33 C. Wang, Y. Ren, Z.-S. Shao, X. Zhao, G.-Y. Zhou, D. Wang, Q. Fang and M.-H. Jiang, *Nonlinear Opt.*, 2001, **28**, 1.
34 *CRC Handbook of Chemistry and Physics*, ed. D. R. Lide, CRC Press, Boca Raton, FL, 73rd edn., 1992–1993.
35 J. N. Demas and G. A. Crosby, *J. Phys. Chem.*, 1971, **75**, 991.
36 M. J. Frisch, G. W. Trucks, H. B. Schlegel, G. E. Scuseria, M. A. Robb, J. R. Cheeseman, V. G. Zakrzewski, J. A. Montgomery, Jr., R. E. Stratmann, J. C. Burant, S. Dapprich, J. M. Millam, A. D. Daniels, K. N. Kudin, M. C. Strain, O. Farkas, J. Tomasi, V. Barone, M. Cossi, R. Cammi, B. Mennucci, C. Pomelli, C. Adamo, S. Clifford, J. Ochterski, G. A. Petersson, P. Y. Ayala, Q. Cui, K. Morokuma, P. Salvador, J. J. Dannenberg, D. K. Malick, A. D. Rabuck, K. Raghavachari, J. B. Foresman, J. Cioslowski, J. V. Ortiz, A. G. Baboul, B. B. Stefanov, G. Liu, A. Liashenko, P. Piskorz, I. Komaromi, R. Gomperts, R. L. Martin, D. J. Fox, T. Keith, M. A. Al-Laham, C. Y. Peng, A. Nanayakkara, M. Challacombe, P. M. W. Gill, B. G. Johnson, W. Chen, M. W. Wong, J. L. Andres, C. Gonzalez, M. Head-Gordon, E. S. Replogle and J. A. Pople, *GAUSSIAN 98 (Revision A.11)*, Gaussian, Inc., Pittsburgh, PA, 2001.
37 T. Helgaker, H. J. Aa. Jensen, P. Jørgensen, J. Olsen, K. Ruud, H. Ågren, A. A. Auer, K. L. Bak, V. Bakken, O. Christiansen, S. Coriani, P. Dahle, E. K. Dalskov, T. Enevoldsen, B. Fernandez, C. Hättig, K. Hald, A. Halkier, H. Heiberg, H. Hettema, D. Jonsson, S. Kirpekar, R. Kobayashi, H. Koch, K. V. Mikkelsen, P. Norman, M. J. Packer, T. B. Pedersen, T. A. Ruden, A. Sanchez, T. Saue, S. P. A. Sauer, B. Schimmelpfennig, K. O. Sylvester-Hvid, P. R. Taylor and O. Vahtras, *DALTON, a molecular electronic structure program, Release 1.0*, 1997.
38 P. Flükiger, H. P. Lüthi, S. Portmann and J. Weber, *MOLEKEL 4.0*, Swiss Center for Scientific Computing, Manno, Switzerland, 2000 .